

Aerodynamic Studies over a Maneuvering UCAV 1303 Configuration

M.S. Chandrasekhara¹ & LT. Brian K. McLain²

Research Professor, Department of Mechanical and Astronautical Engineering
US Naval Postgraduate School, Monterey CA 93943, USA

e-mail: mchandra@nps.edu

Abstract

The flow past and loads on an unmanned combat air vehicle (UCAV) 1303 was investigated in a water tunnel. The UCAV 1303 is characterized by a non-slender, 47-deg swept-leading-edge delta wing, with a cranked trailing edge, a cropped wing tip and a fuselage. It has no vertical tail. Dye visualization and a five-axis strain gage load data were obtained for both steady and unsteady flows, from which body axis force and moment data were derived. Comparison of the flow with slender delta wings showed a number of remarkable differences such as the presence of two like-sense vortices on the same side of the wing, their simultaneous spiral and bubble bursting; as well as some similarities with the slender delta wing behavior. This paper discusses these and also compares the steady flow and unsteady flow results.

I. Introduction

Unmanned Combat Air Vehicles (UCAVs) have already proven effective in many situations in recent times. Their pilotless operation also means that the advantages of aerodynamic phenomena such as dynamic lift can be implemented and effectively exploited for their super-maneuverability and other capabilities. The absence of a vertical tail, control surfaces and a stealthy design has meant that they operate on the fringes of the stability boundary. In fact, studies [1] of the UCAV 1301 - a predecessor to UCAV 1303, the subject of the present research - have shown that like any flying wing, the configuration is unstable. The lack of control authority and stability are both major issues that need to be clearly addressed. Executing unusual maneuvers may cause them to become uncontrollably unstable. Hence, it is critical to understand the aerodynamic behavior of a maneuvering UCAV 1303. Towards this goal, a UCAV 1303 model was tested in the Naval postgraduate School (NPS) water tunnel using dye injection for flow visualization and a 5-component strain gage balance for load data.

The aerodynamic characteristics of conventional delta wings with large sweep angles (above 50 deg) are well known. But, there is only limited flow physics information documented for a non-slender leading edge wing UCAV 1303 type vehicle [2, 3, and 4] despite its popularity with the designers. With the fuselage attached, even less is known and there is virtually no aerodynamics knowledge while they execute maneuvers. For the model with the fuselage OI [5] observed just one instance of a leading edge vortex. There is general consensus that flow over a non-slender wing is only moderately sensitive to Reynolds number, unless the leading edge is rounded. But,

¹ Research Professor

² Lieutenant, US Navy

This paper is declared a work of the U.S. Government and is not subject to copyright protection in the United States

Report Documentation Page

Form Approved
OMB No. 0704-0188

Public reporting burden for the collection of information is estimated to average 1 hour per response, including the time for reviewing instructions, searching existing data sources, gathering and maintaining the data needed, and completing and reviewing the collection of information. Send comments regarding this burden estimate or any other aspect of this collection of information, including suggestions for reducing this burden, to Washington Headquarters Services, Directorate for Information Operations and Reports, 1215 Jefferson Davis Highway, Suite 1204, Arlington VA 22202-4302. Respondents should be aware that notwithstanding any other provision of law, no person shall be subject to a penalty for failing to comply with a collection of information if it does not display a currently valid OMB control number.

1. REPORT DATE OCT 2010	2. REPORT TYPE N/A	3. DATES COVERED -	
4. TITLE AND SUBTITLE Aerodynamic Studies over a Maneuvering UCAV 1303 Configuration		5a. CONTRACT NUMBER	
		5b. GRANT NUMBER	
		5c. PROGRAM ELEMENT NUMBER	
6. AUTHOR(S)		5d. PROJECT NUMBER	
		5e. TASK NUMBER	
		5f. WORK UNIT NUMBER	
7. PERFORMING ORGANIZATION NAME(S) AND ADDRESS(ES) Department of Mechanical and Astronautical Engineering US Naval Postgraduate School, Monterey CA 93943, USA		8. PERFORMING ORGANIZATION REPORT NUMBER	
9. SPONSORING/MONITORING AGENCY NAME(S) AND ADDRESS(ES)		10. SPONSOR/MONITOR'S ACRONYM(S)	
		11. SPONSOR/MONITOR'S REPORT NUMBER(S)	
12. DISTRIBUTION/AVAILABILITY STATEMENT Approved for public release, distribution unlimited			
13. SUPPLEMENTARY NOTES See also ADA540154. Royal Aeronautical Society Aerodynamics Conference 2010. Applied Aerodynamics: Capabilities and Future Requirements. Held in Bristol, United Kingdom on July 27-28, 2010. U.S. Government or Federal Purpose Rights License., The original document contains color images.			
14. ABSTRACT The flow past and loads on an unmanned combat air vehicle (UCAV) 1303 was investigated in a water tunnel. The UCAV 1303 is characterized by a non-slender, 47-deg swept-leading-edge delta wing, with a cranked trailing edge, a cropped wing tip and a fuselage. It has no vertical tail. Dye visualization and a five-axis strain gage load data were obtained for both steady and unsteady flows, from which body axis force and moment data were derived. Comparison of the flow with slender delta wings showed a number of remarkable differences such as the presence of two like-sense vortices on the same side of the wing, their simultaneous spiral and bubble bursting; as well as some similarities with the slender delta wing behavior. This paper discusses these and also compares the steady flow and unsteady flow results.			
15. SUBJECT TERMS			
16. SECURITY CLASSIFICATION OF:			17. LIMITATION OF ABSTRACT
a. REPORT unclassified	b. ABSTRACT unclassified	c. THIS PAGE unclassified	SAR
			18. NUMBER OF PAGES 10
			19a. NAME OF RESPONSIBLE PERSON

it is known that the flow is complex due to the strongly three-dimensional spanwise flow in all cases. For delta wings of low sweep angles, Gursul [2] has provided comprehensive flow details and discussed the differences in leading edge vortex behavior compared to the traditional delta wing flows. Primarily, the vortex is not as dominant and its breakdown is far less clearly discernible, [Ol, 5]. Significant spanwise flow develops in the low sweep angle case like that typically seen in yawed wings which affects the formation and behavior of the vortex. As a result, the vortex forms at a very low angle of attack and bursts diffusely at lower angles unlike slender delta wing vortices causing lift and moment breaks. Additionally, Cummings et al [1] have verified an observation by Cunningham ([6] that over a pitching UCAV 1301 model that pitch-breaks are a major feature which is attributable to the vortex behavior. Wong et al [7] show that tip stall can occur in these configurations which can initiate the pitch-break. McLain [8] and Chua [9] also documented some flow details in this flow and found reasonable support for these results.

The above mentioned studies for most part addressed some general aspects of the flow. Whereas a slender delta wing flow is dominated by large, conical leading edge vortices that are primarily responsible for the enhanced lift observed, the corresponding vortices in the non-slender wing case are not so well defined. If present, they also can be expected to contribute to some lift (and its loss) depending on the angles of attack of their formation and breakdown. The slender delta wing flow vortices form at angles of attack around 10 degrees and higher as the vortical boundary layer rolls up from the wing underside and separates along the leading edge. But, the results are neither as clear nor as definitive for the non-slender wing flow. A dual-vortex structure has been observed by Taylor, et al [4], Ghee and Hall [10]; it appears to be also elongated [1]. The vortices have the same sign, unlike the primary vortex and the induced secondary (and sometimes tertiary) vortices each of which has opposite signs in the slender wing flow. The vortices appear to remain close to the surface of the non-slender delta wing even at moderate angles of attack indicating a strong viscous/inviscid interaction. In addition, the vortices have been known to move away from or towards the wing central plane. The vortices also can breakdown at low angles of attack. Evidence of tip stall has been found in some studies [7 and 8]. Such events may give rise to unacceptable lift and pitching moment breaks that have been observed. In fact, Ref. [10] states that a break in lift occurs at a very low angle of attack, $\alpha = 2.5$ deg as well as at a few other higher angles of attack. The moment-breaks can lead to potentially hazardous instabilities.

The benefits of dynamic stall and the extra lift are important at all flight speeds and are well documented [11]. With the human out of the cockpit, the UCAV can be designed to exploit these benefits by making it perform unusual maneuvers. Dynamic lift during a maneuver can be especially valuable while evading a perceived threat. If the flow can be suitably controlled, to mitigate the undesirable effects by passive means, it can become a viable option for the UCAV. The overall study is deeply concerned with establishing the maneuver aerodynamics of the UCAV about which little is known presently so that a superior vehicle is available for national defense.

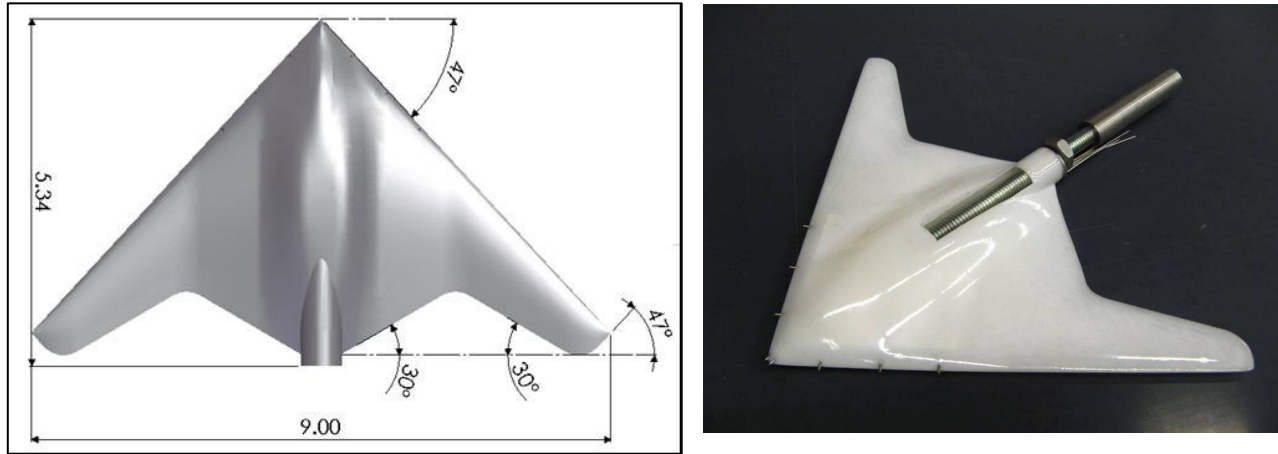


Fig.1. UCAV 1303 model with dimensions (inches), and dye-ports as used in the NPS water tunnel

Towards this goal, a blended wing-body UCAV model was studied in the NPS water tunnel. So, one could expect to see some of the above described flow characteristics and additional ones due to presence of the fuselage. This paper details some of the commonalities and differences observed when compared to the plain non-slender wing flow.

II. Description of the UCAV 1303 Model and Experiment

The UCAV 1303 geometry used for the tests, shown in Fig. 1, was provided by the US Air Force. Two 1:72 scaled models (of dimensions shown) were built for this investigation; one for flow visualization and the other for load data using a five-component strain gage balance. The models were fabricated using rapid prototyping techniques and had smooth polyurethane coat finish. The fuselage was also included in the geometry. It had a leading edge sweep of 47° , the trailing edge was cranked with a sweep of $\pm 30^\circ$ and $\pm 47^\circ$. Both models were identical in planform area, span and mean aerodynamic chord (265 cm^2 , 22.86 cm , and 13.56 cm respectively).

The flow visualization model was solid and contained eight symmetrically located dye ports, 0.6 mm in size, placed at $0.01c$, $0.11c$, $0.22c$ and $0.33c$; two of these placed to capture the critical region of wing body junction. The dye tubes were routed through the model interior. Additionally, a movable dye tube was located underneath the starboard leading edge outside of the model. Side views and top views of the flow were captured using synchronized, software triggered digital cameras.

The load study model was fabricated in two pieces and housed a water-proofed internal balance to measure normal force (N), side force (S), pitching moment (PM), rolling moment (RM) and yawing moment (YM). The two-piece design facilitated placement of the internal balance at the aerodynamic center and ensured proper fit.

Both steady flow data and detailed phase-locked flow visualization images were obtained as also ensemble averaged (typically 20 runs) load data while the model executed specific maneuvers. Typical maneuvers were simple pitch-up at different rates and freestream speeds, simple roll-maneuvers at zero angle of attack, and similarly, simple yaw- maneuvers. Some roll-maneuvers at different rates for non-zero angles of attack were also carried out. A movie of the dye-flow was obtained at a very slow pitch rate while pitching from 0 – 30 deg (to represent a nearly steady state conditions) to see the flow evolution with angle of attack.

III. Results and Discussion

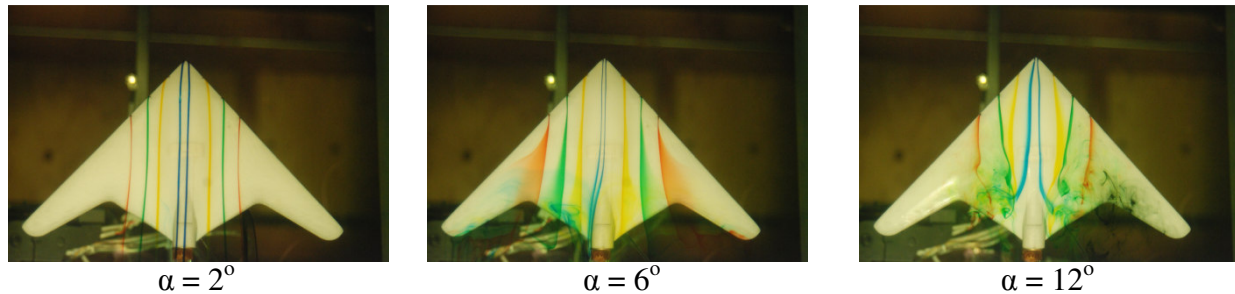


Fig. 2. Flow at $U_\infty = 5$ cm/s, $Re=3,800$

Steady flow images are presented in Fig. 2 for a velocity of 5 cm/s, $Re = 3800$. These images show near perfect symmetry of the flow over the wing, with the streamlines slight curving towards the wing tips. Side views of the flow clearly showed that the dye split at the wing leading edge between the upper and lower surfaces. Both streams flowed straight into the wake which is remarkable in itself because based on slender wing knowledge, one expects the flow to move wrap around the leading edge or on the basis of a yawed wing, it should move spanwise. As the angle of attack increases, the flow symmetry is retained, but significant dye spreading occurs near the trailing edge crank – the red dye at $\alpha = 6^\circ$. As the flow has not yet separated, the pattern seen to represent the surface flow features. A slight pooling of the blue dye was seen near the sting at $\alpha = 2^\circ$ (not shown); it is believed to be due to the larger diameter of the fuselage due to engine housing at this location (see also Fig. 3). Even with outward spreading of the dye on the upper surface at $\alpha = 6$ deg, dye traces could be distinguished on the lower surface. At a higher angle of attack ($\alpha = 8$ deg), definite leading edge vortices become visible and for $\alpha = 12$ deg shown, the vortices burst at about three-quarter-chord downstream of leading edge. Even as the yellow dye seems to move parallel to the fuselage and the nose tip flow moves away from the fuselage at $x/c \approx 0.7$, the flow from the outboard locations moves *towards* the fuselage unlike what was seen for at $\alpha = 6$ deg. These trends were seen at higher Reynolds numbers also suggesting that the delta wing vortex structure does not behave as it would in a slender delta wing.

A full sequence of the flow is presented in Fig. 3 for a higher freestream flow condition, $U_\infty = 15$ cm/sec and $Re = 11,700$ which enables a full flow review at various angles of attack. By $\alpha = 2^\circ$, it is possible to see some spanwise flow at the trailing edge from the back of the fuselage. At $\alpha = 4^\circ$, the presence of the red-dye at the starboard wing tip points to the onset of mild tip-stall. But, the flow is well behaved ahead, toward the front of the wing. By $\alpha = 6^\circ$, tip-stall is clear and the outboard wing dye pattern appear like the footprint of the vortex. As stated earlier, the dye does not migrate too far above the surface indicating a strong viscous/inviscid interaction and

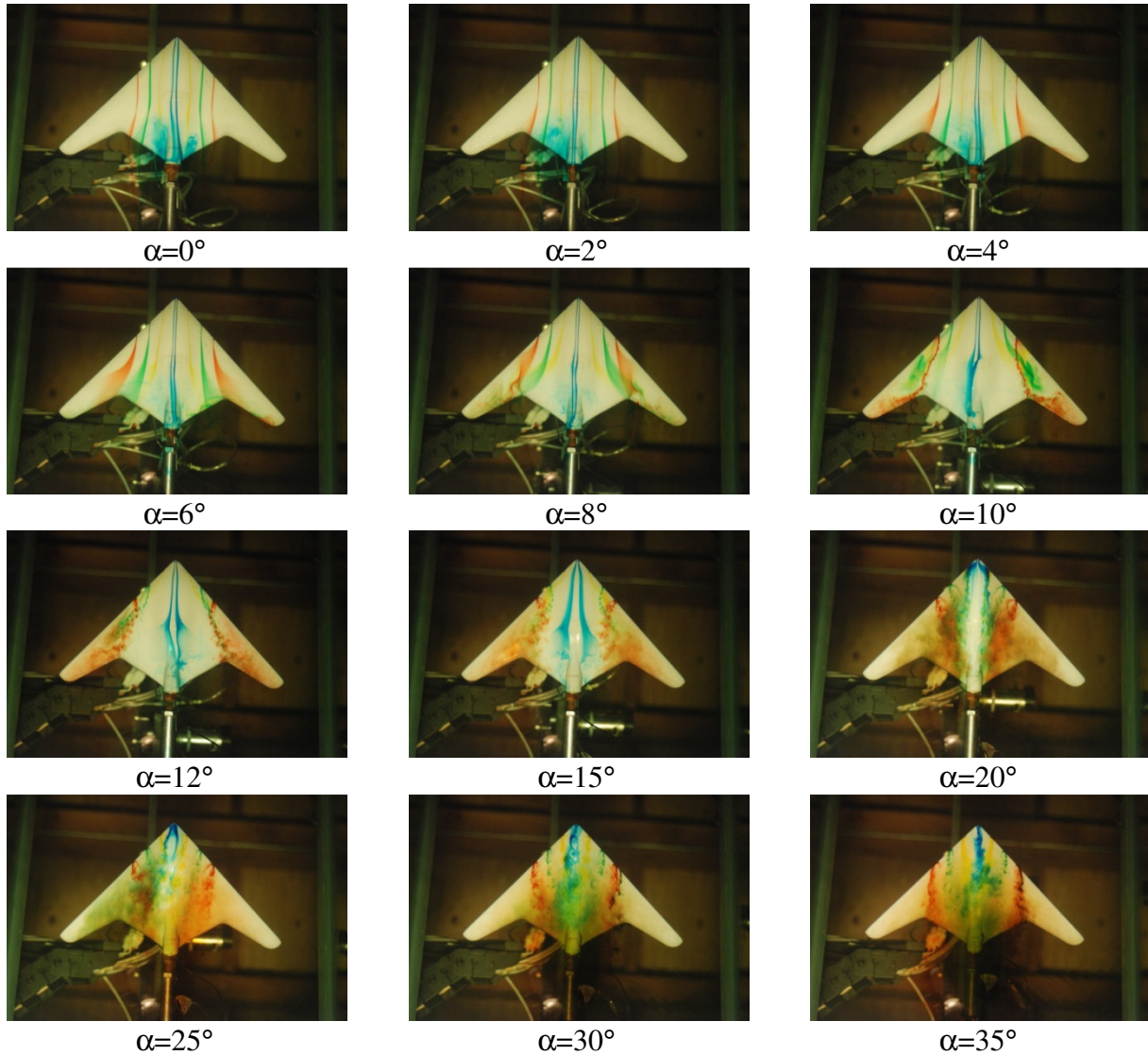


Fig. 3 Flow over UCAV 1303, $U_\infty = 15 \text{ cm/s}$, $Re = 1.17 \times 10^4$

essentially, provides the surface flow pattern here. However, its shape does not resemble the familiar delta wing associated surface flow pattern. Interestingly, the pattern compares almost perfectly with the computed surface shear flow pattern presented by Petterson [12] for a Mach number of 0.25, $\alpha = 12^\circ$ and at a much higher Reynolds number, Fig. 4. This lends credence to the method of using a water tunnel for such investigations.

In an attempt to better understand the flow evolution, a video of the flow was recorded as the model was pitched from $\alpha = 0^\circ$ to $\alpha = 30^\circ$ at a very slow rate to be essentially steady flow. To verify if the bottom surface flow wraps around the leading edge, black dye was introduced from this side. It seemed to flow straight into the wake until a higher angle of attack. The video clearly showed that following tip stall and local effects including flow reversal, the tip stall grew in size and engulfed the outboard regions of the wing. The topology of the surface flow is quite complex and despite tip-stall outboard, the wing-body junction flow (yellow dye) and the nose-tip flow

(blue dye) are only affected at $\alpha = 6$ deg. Between $\alpha = 6^\circ$ and $\alpha = 8^\circ$, a tightly coiled vortical structure appears. Complex surface flow interactions can be seen at $\alpha = 8^\circ$. However, by $\alpha = 10^\circ$, the primary vortex breaks down. The location of the breakdown point moves upstream towards the leading edge as the angle of attack is increased. Unlike a slender delta wing flow, a nose-tip vortex also is seen on the fuselage. Both these vortices have the same sign. The nose-tip vortex experiences a bubble-type breakdown (see Fig. 4) at around 50% of the fuselage length over a small range of angles of attack ($10^\circ < \alpha < 15^\circ$). The observation of two different breakdown mechanisms simultaneously is indeed intriguing. This intricate flow pattern is new and has not been reported earlier on this configuration. Up to $\alpha = 12^\circ$, the flow generally exhibited a tendency to flow outboard. However, after that an inboard movement was observed. Upon further review of the video at this angle of attack, it became clear that the tip stall flow moving upstream had acquired a strong spanwise velocity and moved rapidly towards the nose tip of the aircraft. It just moved parallel to the leading edge (see Fig. 5) but, did not get engulfed by the primary vortex as generally seen for large sweep angles. Some traces of tip-stalled flow were also being shed into the tip-wake region.

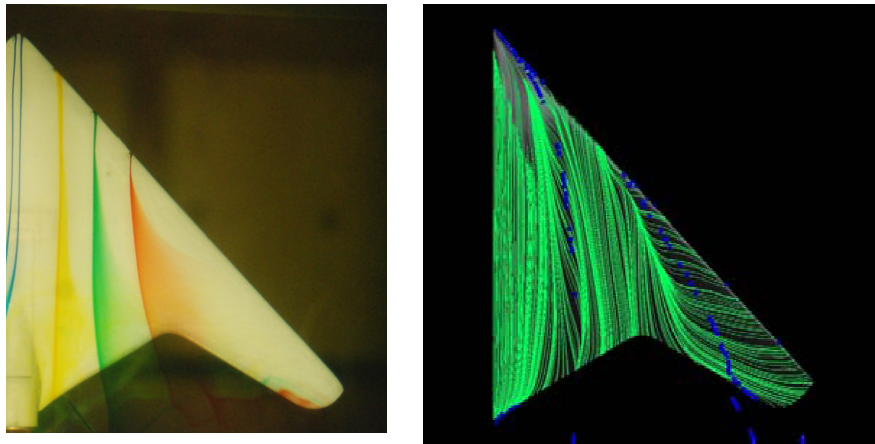


Fig. 4: Experiments $Re = 3.8 \times 10^3$; Right: $M=0.25$, $\alpha = 10^\circ$
 $Re=1.6 \times 10^6$ (AIAA-2006-1259, Petterson)

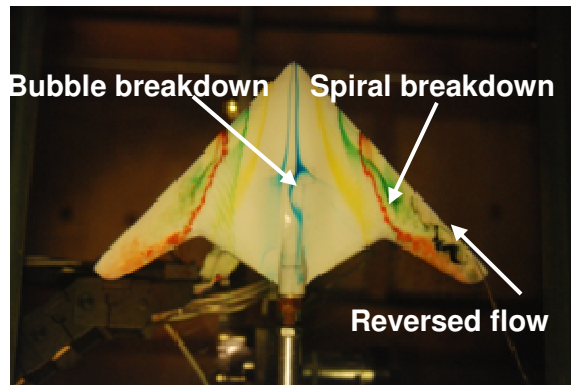


Fig. 5. Spiral and bubble type breakdown phenomena, $\alpha=10^\circ$, $U_\infty= 15$ cm/s

The vortex once formed exhibited a dependence on Reynolds number similar to what was observed in case of slender delta wings as shown in Fig. 6.

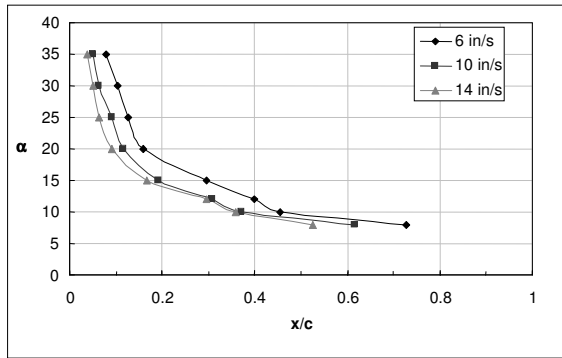
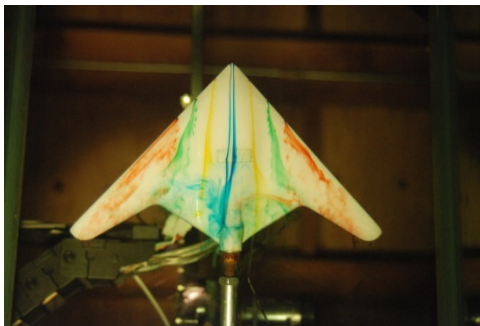
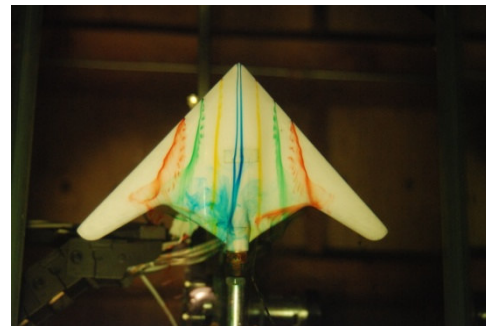


Fig. 6. Reynolds number dependence of vortex breakdown. In addition, roll and yaw maneuvers were carried out at roll rates of 3deg/s, 5deg/s and 7deg/s. Various combinations were tried and only a few specific cases are discussed below.

For pitch up cases, the result of delay of vortex breakdown with increasing pitch rate and relative to steady flow case that has been well documented for delta wings was observed here also, even though the formation of the vortex did not occur in a similar manner. Likewise, pitch down yielded accelerated rates of breakdown.



Pitch Rate, $\dot{\alpha}=3^\circ/s$



Pitch Rate, $\dot{\alpha}=7^\circ/s$

Fig. 7. Combined pitch-roll maneuver, $U_\infty=6$ [in/s], $Re=1.17 \times 10^4$, $\alpha=10^\circ$, $\phi=10^\circ$; Roll to starboard side

The model was set to steady roll angles and pitched from 0 to 30 deg at rates of 3deg/s and 7deg/s. The yaw angle was maintained at zero deg. The results are shown in Fig. 7. During this combined maneuver investigation, Fig. 7 shows that at an angle of attack of 10 deg and a roll angle of 10 deg, LEV formation is observable. The higher pitch rate, as with the pitch only maneuver case investigated, has significantly delayed vortex formation and bursting, lowered the amount of flow separation along the outer wing regions and reduced wing tip stall. The wing flow typically moves towards the upper wing tip as seen here also which is likely to induce tip-stall on the port side for this case. However, the starboard tip stall is relieved and it is clearly seen that the flow is moving towards the fuselage from the crank instead of towards the tip.

Yaw maneuver studies at a fixed pitch angle of zero deg indicated the presence of strong side-slip like that was observed for steady flow cases. No other effects could be seen. These may appear as the angle of attack and roll angle are increased.

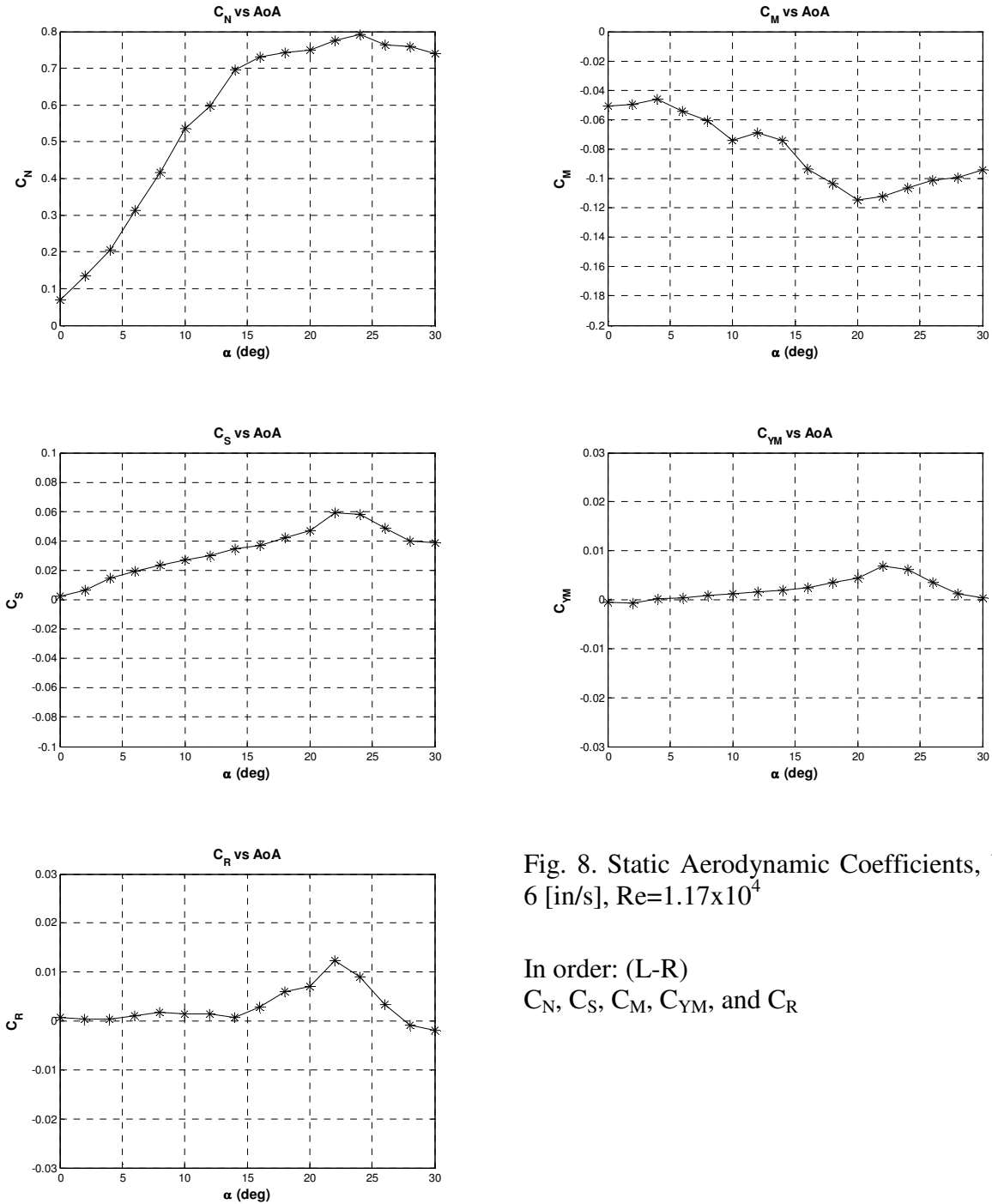


Fig. 8. Static Aerodynamic Coefficients, $U_\infty = 6$ [in/s], $Re=1.17 \times 10^4$

In order: (L-R)
 C_N , C_S , C_M , C_{YM} , and C_R

Load and moment (representative) data shown in Fig. 8 indicates that there are noticeable changes in the slope of C_N with angle of attack. A small change is seen around $\alpha = 4^\circ$, which

corresponds to the observed tip-stall. Subsequently, an increase is seen which corresponds to the formation of the vortex. At $\alpha = 11^\circ$ a drop is noted, which correlates reasonably with vortex bursting as it begins to affect the loads on the wing. At higher angles, the slope levels off. Correspondingly, the pitching moment also varies with noticeable breaks around these angles. Some differences can be seen, which are believed to be due to the extremely low load levels in water tunnel studies (a few grams) directly. A very slight increase can be seen in both the side force and yawing moment until the vortex bursting event occurs when the values become reasonably large. A steep rise in the rolling moment can be seen when the vortex first forms and then again after $\alpha = 12^\circ$ to $\alpha = 15^\circ$. The latter is directly attributed to the asymmetric and unsteady vortex bursting. In an experiment to ascertain this feature, several observations were recorded at each of angle of attack over the range where vortex bursting was present. It was clear that the vortex burst asymmetrically and on each side, the location itself moved unsteadily along the wing chord by as much as 10-15% depending on angle of attack. Some distinct spanwise movement was also noticed as the leading edge separated flow wandered. These can be expected to give rise to the trends noted in Fig. 8.

IV. Concluding Remarks

Flow visualization and load measurements over a UCAV 1303 model in a water tunnel were obtained for a large experiment matrix from which a limited set of results are selectively presented. Some unusual flow features were observed, which are different from the ones reported in the literature. The model stalled first with tip-stall occurring at a very low angle of attack. This manifested in a normal force break at the corresponding angle of attack. The cause of tip-stall appeared to be the spanwise outboard flow from near the fuselage towards trailing crank. This may have inhibited the vortex from forming in a manner well known for a slender delta wing. The upstream, spanwise flow near the leading edge from the tip-stall flow caused the surface flow pattern to take on a steep curved pattern. Subsequently, the leading edge flow separated to form a vortex. The vortex appeared to be tightly wound and small, stayed close to the upper surface, but burst quickly at low angles of attack (10-12 deg) unlike a slender delta wing. Prior to its formation, the flow just detoured around the spanwise flow mentioned above and spread towards the wing tip. However, when the vortex began to burst, the flow curved towards the fuselage. This rapid movement of the flow may have been responsible for some unexpected loads. Pitching the model at different rates yielded results similar to the slender wing cases by delaying vortex breakdown. Increasing Reynolds number moved vortex bursting at a given angle towards the trailing edge. Rolling at different rates had a similar effect, this time also help alleviate tip stall on the wing tip that went up. Early load data followed these trends well.

Acknowledgements

Funding support for the project (TDSI/07-005/1A) was provided by the Singapore TDSI/Temasek Group under a CRADA with the US Naval Postgraduate School. This is gratefully acknowledged. The authors express their thanks to the USAF for supplying the model geometry file.

V. References

1. Cummings R.M. Morton S.A and Siegel S.G. Numerical prediction and wind tunnel experiment for a pitching unmanned combat air vehicle. *Aerospace Science and Technology*, Vol. 12, pp. 355-364, 2008.
2. Gursul I. Gordnier R and Visbal M. Unsteady aerodynamics of nonslender delta wings. *Progress in Aerospace Sciences*, Vol. 41, pp. 515-557, 2005.
3. Yaniktepe B and Rockwell D. Flow structure on a delta wing of low sweep angle. *AIAA Journal*, Vol. 42, No. 3, pp. 513-523, 2004.
4. Taylor G.S. Schnorbus T and Gursul I. An investigation of vortex flows over low sweep delta wings. *AIAA 33rd Fluid Dynamics Conference and Exhibit*. Orlando, FL, USA, AIAA 2003-4021, Jun. 2003.
5. M.V. Ol, "Water Tunnel Velocimetry Results for the 1303 UCAV Configuration AIAA-2006-2990, 2006.
6. A.M. Cunningham, Jr., T. Bushlow, *AIAA-90-2815-CP*, 1990.
7. D.W. Wong, G.J. McKenzie, M.V. OL, K. Petterson, S. Zhang, *AIAA2006-2984*, 2006.
8. McLain, B.K. "Steady and Unsteady Aerodynamic Flow Studies over a 1303 UCAV Configuration" *MS Thesis*, US Naval Postgraduate School, Sep. 2009.
9. W.H. Chua, "Flow visualization studies over a UCAV 1303 model" *M.S. Thesis*, Naval Postgraduate School, 2009.
10. Ghee T.A and Hall D.R. Experimental and numerical investigation of vortex shedding of a representative UCAV configuration for vortex flow control, *Proc. RTO AVT Symposium on Advanced Flow Management: Part A- Vortex Flows and High Angle of Attack Military Vehicles*, Loer, Norway, RTO-MP-o69(I), May 2001.
11. Carr, L.W. and Chandrasekhara, M.S. "Compressibility Effects on Dynamic Stall", *Progress in Aerospace Sciences*, Vol. 32, pp. 523-576, 1996
12. Petterson K. CFD analysis of the low-speed aerodynamic characteristics of a UCAV. *AIAA 44th Aerospace Sciences Meeting and Exhibit*. Reno, NV, USA, AIAA 2006-1259, Jan. 2006